Boletim da Sociedade Astronômica Brasileira, **35**, no. 1, 95-98

Simulations of the H Balmer series in solar flares

Gabriel F. S. Silva[1], Paulo J. A. Simões[2], Christopher Osborne[3], Adam F. Kowalski[4], Graham Kerr[5], & Lyndsay Fletcher[6]

[1] Universidade Presbiteriana Mackenzie, Escola de Engenharia e-mail: 72257261@mackenzista
[2] Universidade Presbiteriana Mackenzie, CRAAM e-mail: paulo.simoes@mackenzie.com
[3] University of Strathclyde e-mail: christopher.Osborne@glasgow.ac.uk
[4] University of Colorado Boulder, Department of Astrophysical and Planetary Sciencese-mail: adam.f.kowalski@colorado.edu
[5] The Catholic University of America, NASA Goddard Space Flight Center, Greenbelt Md e-mail: raham.s.kerr@nasa.gov
[6] University of Glasgow, SUPA School of Physics and Astronomye-mail: lyndsay.fletcher@glasgow.ac.uk

Abstract. Observations of high-order Balmer series lines during flares are rare, despite their great usefulness for diagnosing electron density in the solar chromosphere during flares, as predicted by theoretical studies. The study of the Balmer series is also relevant due to its spectral proximity to the Balmer continuum and studies of the origin of the *white-light* emission in flares. We aim to analyze the spectrum of the Balmer series of hydrogen, focusing on high-order lines, during solar flares, through radiative-hydrodynamic (RHD) simulations. Its observational characteristics, such as relative and absolute intensities, will be studied as a function of energy deposition in the solar chromosphere. We are employing a database of RHD simulations, created by the European project F-CHROMA, with dozens of models describing the evolution of the solar atmosphere during flares from different energetic conditions. The resulting spectra will be used in future projects under development at CRAAM: verification of the detectability limits of a new spectrometer for solar observations, and in the study of stellar flares. The new simulations will be made freely available to the scientific community, to be used in the investigation of solar and stellar flares.

Resumo. Observações das linhas de alta ordem da série de Balmer durante flares são raras, apesar de sua grande utilidade para o diagnóstico da densidade de elétrons na cromosfera solar durante flares, prevista por estudos teóricos. O estudo da série Balmer é também relevante devido à sua proximidade espectral com o contínuo Balmer e estudos da origem da emissão *white-light* em flares. O objetivo desta proposta é analisar o espectro da série de Balmer do hidrogênio, com foco nas linhas de alta ordem, durante flares solares, através de simulações radiativo-hidrodinâmicas (RHD). Suas características observacionais, como intensidades relativa e absoluta, serão estudadas em função da deposição de energia na cromosfera solar. O espectro Balmer será gerado usando ferramentas para o cálculo da geração e transferência radiativa, partindo de um banco de simulações RHD, criado pelo projeto europeu F-CHROMA. Este banco conta com dezenas de modelos descrevendo a evolução da atmosfera solar durante flares a partir de diferentes condições energéticas. Os espectros resultantes serão usados em futuros projetos em desenvolvimento no CRAAM: verificação dos limites de detectabilidade de um novo espectrômetro para observações solares, e no estudo de flares estelares. As novas simulações serão disponibilizadas livremente para a comunidade científica, para serem usadas na investigação de flares solares e estelares.

Keywords. Sun: activity – Sun: flares – Methods: numerical

1. Introduction

Solar flares are believed to be the result of the conversion of magnetic energy into particle kinetic energy. The energy released in flares is about 10^{27}–10^{32} erg, a large fraction of which is in the kinetic energy of accelerated, non-thermal electrons and ions, as estimated of hard X-rays and emission of γ rays, e.g., Emslie et al. (2012). Part of the energy released is radiated as thermal emission in soft X-rays from the corona, line emission and continuum in the ultraviolet from the chromosphere and transition region (chromosphere/corona) and white light (optical continuum) observed of the chromosphere or photosphere (Milligan et al 2014).

Observations of high-order Balmer H series lines during flares are rare; Here we highlight unique examples discussed by Fritzová-Švestková et al (1967) and Procházka et al (2017). In the 1960s, the idea of obtaining a diagnosis of electron density was proposed by measuring the width of high-order lines (above H9) of the Balmer series of H (Fritzová-Švestková et al 1967). The method assumes constant electron temperature and that the high-order lines are in the optically thin regime. Electron densities of the order of 3×10^{13} cm^{-3} in flares were obtained by this method, with uncertainties of the order of 30% (Fritzová-Švestková et al 1967); such values for electron density were used for analysis and discussion of the formation of WLFs (Machado et al 1974; Neidig 1983). Procházka et al (2017) presented observations of the H Balmer series during two intense solar events. These observations were the result of a unique observation campaign with a spectrometer installed at the Ondrejov Observatory (Kotrˇc et al 2016), in the Czech Republic, and is no longer in operation. However, these observational results indicate the importance of including the Balmer series in studies of the optical spectrum of solar flares.

Observations of the Hα line in conjunction with other lines in the Balmer series are practically non-existent. The only observation of a flare in Hα and Hβ, simultaneously, was presented by Capparelli et al (2017). Simultaneous observations of the Hα and Hβ lines allowed the first analysis of the relative intensity of the respective emissions. However, spectral analysis was only possible for Hα, as the emission in Hβ was obtained with a line-centered narrow filter imager. A more in-depth analysis was only possible through the employment of radiative hydrodynamic simulations.

Flares in active stars have been detected for many decades through dedicated observations, which, although lacking spatial resolution, generally provide good coverage and/or spectral resolution Hawley et al (1991, 2003). Naturally, the knowledge acquired about solar flares is directly used for the interpretation of

stellar flares. The detection of stellar flares has become more frequent with the operation of telescopes such as the *Kepler Space Telescope*. We emphasize that stellar flare spectra, with high resolution in the visible range, are relatively common, which allows a more detailed study of the formation of the flare spectrum (Kowalski et al. 2013). However, due to the lack of spatial resolution in stellar observations, it is impossible to distinguish the relative contributions of the different active structures during flares, encouraging the use of *multi-thread* models, as for example used by Kowalski et al. (2017) for the study of the *megaflare* observed in the star YZ CMi.

Despite the many differences between solar and stellar flares, the former remain the models on which interpretations are based (Namekata et al 2017). Although their main mission is the search for exoplanets, telescopes such as *Kepler Space Telescope* and *Transiting Exoplanet Survey Satellite* (TESS) have provided a vast amount of data on stellar flares (Okamoto et al 2022), detected with excellent photometry using broadband filters in the visible range. Flares in stars observed in visible light are typically modeled as a blackbody at 10^4 K (Maehara et al 2012). We understand that this model is not physically suitable (Simões et al 2024), for the same reason mentioned above that the blackbody mechanism is not suitable to explain the optical continuum in solar flares. The results of this project will be fundamental for interpreting stellar flares detected by broadband instruments as a manifestation of the hydrogen recombination spectrum, based on the inclusion of the contribution of spectral lines from the Balmer series of H.

The use of radiative-hydrodynamic (RHD) simulations as a tool for investigating solar flares makes it possible to study the energetic transitions (excitation, ionization and recombination) in the ions present in the plasma during the events, where plasma heating occurs and evaluate energy transport mechanisms. Such tools have become fundamental for understanding plasma physical processes that cannot be directly observed, and also for exploring and predicting the radiation spectrum of solar flares for bands of the electromagnetic spectrum with little or no coverage by operating telescopes - such as This is the case of the recombination limit region and the high order lines of the Balmer series.

In this work, our objective is to present preliminary results of our study of the characteristics of high-order lines in the Balmer series as a function of the energy deposited in the atmosphere. To achieve the objectives, using synthetic spectra generated in RHD simulations.

2. RHD simulations

To achieve the proposed objectives, the methodology is based on the analysis of synthetic spectra generated from the evolution of the solar atmosphere during flares through radiative-hydrodynamic simulations and radiative transfer from the Balmer series to H19.

Our knowledge of the structure of the solar atmosphere is fundamentally based on one-dimensional semi-empirical models (e.g. Vernazza et al 1981; Fontenla et al 1983) and in flares (Machado et al 1980, e.g.). Such semi-empirical models have been extremely useful in several topics in Solar Physics. However, the solar chromosphere is not static, especially during flares. Radiative-hydrodynamic (RHD) simulations have been used for many years to model the dynamics of the solar atmosphere during flares (Allred et al 2015), and have become increasingly popular and useful given the advancement of computational techniques, more precise physical descriptions and, mainly, the increase in processing power over the years. Fundamentally, such simulations are based on calculations of the plasma hydrodynamics of the solar chromosphere, when subjected to energy deposition processes and radiative losses. The radiative processes in the plasma are relevant to the thermodynamic equilibrium of the plasma, therefore, radiative transfer calculations are also necessary, including processes of excitation, ionization and recombination of the main atomic species in the plasma.

In this project we will use simulations with the code `RADYN` (Carlsson et al 1995) adapted for flare modeling (Allred et al 2005), which has been the subject of constant development (Allred et al 2015). The `RADYN` code numerically solves the coupled equations of hydrodynamics, radiative transfer and atomic level transitions of the elements H (6 levels), He (9 levels) and Ca (6 levels) in a self-consistent way and as a function of time, for a plane-parallel atmosphere of one dimension, and outside the local thermodynamic equilibrium (*non-local thermodynamic equilibrium*, NLTE). The choice of atomic species (and their transitions) was based on their energetic relevance and their opacities. The main energetically relevant transitions of other species are calculated assuming conditions in local thermodynamic equilibrium (*local thermodynamic equilibrium*, LTE), with a significant reduction in computational cost. The `RADYN` code produces height profiles of several properties of the solar atmosphere, including temperature, electron density, density of H, He, and Ca (for each level of excitation and ionization considered), pressure, macroscopic velocity vertical, among other characteristics. The code also simulates the emission of several spectral lines and recombination continua that are important for the energy balance of atmospheric plasma.

Energy transport and deposition is based on the most accepted assumption that electron beams accelerated in the solar corona carry and deposit in the plasma the most important fraction of the energy in a flare (Fletcher et al 2011). In the most recent version of the `RADYN` code, the transport and deposition of energy is done by solving the electron distribution function in energy, pitch angle, position and time, described by the Fokker-Planck formulation (Allred et al 2020).

The production of RHD models of flares demands high computational resources and time, in addition to being a highly specialized task. With this in mind, we will use a bank of solar flare models[1] using the code `RADYN` (Carlsson et al 2023). The bank was created by the project *Flare Chromospheres: Observations, Models and Archives* (F-CHROMA)[2]. This model database was created with the aim of facilitating the comparison of models with observations and promoting a greater understanding of the physics of the chromosphere during flares. The model database has more than 79 simulations generated for different parameters of energy deposition in the solar atmosphere.

2.1. F-CHROMA model database

The models consider an injection of energy by deposition of accelerated electrons, parameterized as a power law distribution, in terms of its spectral index δ and the lower energy limit E_0. The energy injection is modeled by a triangular pulse of 20 seconds duration, with total energy $E_{\rm tot}$. These parameters, listed in Table 1, were combined to form a total of 96 scenarios. We note that 17 scenarios did not converge numerically and are therefore not available. The 79 models available in the F-

[1] Available at `https://star.pst.qub.ac.uk/wiki/public/solarmodels/start.html`

[2] The F-CHROMA project was funded by the European Community's Seventh Framework Programme, `https://cordis.europa.eu/project/id/606862`

Table 1. Electron beam parameters in the RADYN F-CHROMA simulations.

Parameter	Symbol	Value
Spectral index	δ	3, 4, 5, 6, 7, 8
Total energy	$E_{\rm tot}$(erg/cm^2)	3×10^{10}, 10^{11}, 3×10^{11}, 10^{12}
Energy cut-off	E_0 (keV)	10, 15, 20, 25

CHROMA database are considered numerical experiments to assist in the interpretation of observational data and the study of flare physics, taking care not to interpret the simulation results as a faithful portrait of reality.

2.2. Lightweaver

The calculation of the radiative transfer of optically thick spectral lines under NLTE conditions is one of the most computationally demanding problems in the study of the physics of solar and stellar flares. Such a calculation consists of, from an atmosphere model, computing the atomic populations in a self-consistent way while taking into account how the radiation originating from atomic transitions can alter such populations. The computational cost derives from the high number of dimensions involved in calculating radiation intensities: wavelength, space, time, and direction of radiation propagation.

One of the main tools used in solar physics to calculate radiative transfer is the RH (Uitenbroek 2001) code, although its use is limited due to its high complexity of operation. Recently, a new tool was proposed with the aim of promoting greater flexibility and access to this area of study: Lightweaver (Osborne et al 2021). With its *front-end* written in Python language (giving access to the high-performance *back-end* written in C++), this new tool is available to the scientific community offering the same advantages as RH code but with a lower access barrier. Other advantages is that one of its developers also created the module radynpy[3], to access RADYN file in Python, with easy integration with Lightweaver. The tool also uses the same file format for atomic models as RH, ensuring access to resources already developed and tested by the community. In particular, an atomic model of H with 20 levels is available, allowing the synthesis of spectral lines up to H19 (Kowalski et al. 2017, 2022). Other advantages offered are increased computational performance of calculations, greater reliability of the numerical core, performance gains through optimized and specialized methodologies and its ability to generate documents in HTML and LaTeX (Osborne et al 2021).

2.3. Synthesis and analysis of Balmer series spectra

The methodological sequence for producing Balmer series spectra for solar flares simulated in the F-CHROMA model database is as follows: 1. choice of hydrogen atomic model with 20 energy levels in Lightweaver; 2/ definition of the wavelength range for spectrum calculations: 365 to 405 nm in Lightweaver; 3. reading the F-CHROMA model file via radynpy; 4. spectrum calculation via Lightweaver for the atmosphere at each time step; 5. the synthesized spectra are archived sequentially in files in the format *comma separated values* (csv).

In order to check the effects of energy deposition parameters (i.e. accelerated electron beam, spectral index δ, lower cutoff energy E_0 and energy flow F, see Table 1) in the formation of the Balmer series, we will analyze the absolute and relative intensities of the H series lines as a function of the energy deposition parameters, as well as the analysis of how these lines accumulate close to the Balmer continuum and seek physical explanations for the results obtained. In the following section we present some preliminary results obtained.

[3] https://github.com/Goobley/radynpy

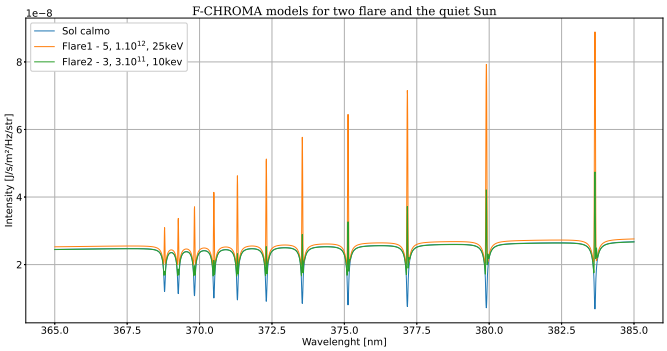

Figure 1. Simulated Balmer spectra for models 7 and 69, compared to the quiet Sun spectrum.

3. Preliminary results

3.1. Balmer series spectra

As a result of the first simulation involving a solar atmosphere model from the F-CHROMA model database, we obtained a synthetic spectrum from Model 12, which has the characteristics $\delta = 8$, $E_0 = 10$ keV, and total energy flow= 3×10^{11} erg/cm^2. All the spectra produced was generated both for the flare and for the spectrum of the quiet Sun, with wavelengths varying between 365 and 385 nm, corresponding to the continuous and high lines order of the Balmer series.

The spectrum of the Sun was generated in conjunction with the flare for comparison purposes in order to highlight the magnitude of the intensity and emission produced by the flare, as well as verify which lines presented substantial emission.

The model we used showed low emission in high order lines, showing little and almost no emission, which only becomes evident from line H15, and which continues to increase in the following lines, which present emission in a very narrow line. The spectrum also showed an increase in intensity in regions where emissions do not occur due to continuous emission from hydrogen recombination present in the atmosphere.

To carry out the comparative analysis between relative and absolute intensities, we obtained the spectra of high-order Balmer lines for two different models from the F-CHROMA database with the following characteristics: Model 69: $\delta = 5$, $F = 1{,}0\times10^{12}$ erg/cm^2, $E_0 = 25$ keV and Model 7: $\delta = 3$, $F = 3{,}0\times10^{11}$ erg/cm^2, $E_0 = 10$ keV. It is interesting to note that other simulated models did not produce noticeable changes in the high-order Balmer lines.

The resulting spectra are presented in Figure 1, it presents Flare 1 (model 69) and Flare 2 (model 7), and as a comparison measure the quiet Sun, as a function of the length of analyzed wave and emission intensity.

The high-order lines of Flare 1 presented profiles partially in emission, while for Flare 2 the lines did not show great variation in relation to the spectrum of the quiet Sun. We also did not notice a large increase in the continuum, but we have not yet carried out a quantitative analysis.

To better visualize the change in the Balmer lines, we subtracted the contribution of the quiet Sun spectrum from each

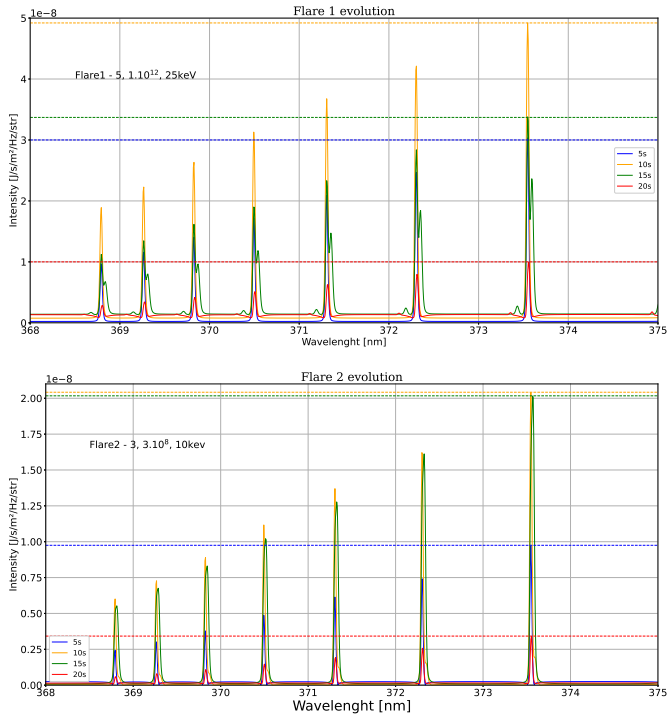

Figure 2. Evolution of the emission produced by Flare 1 and 2 during the time intervals of the triangular energy injection pulse for time intervals of 5 seconds

simulated spectrum, obtaining the excess emission in the simulated flares. These results are in Figure 2, comparing their intensity. For comparison purposes, we limited the wavelengths to between 365 and 375 nm, favoring the visualization of high-order lines, especially the absolute intensity of the emission from Flare 2, which was considerably lower compared to Flare 1. This difference in intensity, with Flare 1 (model 69) greater than Flare 2 (model 7), is probably related to the greater energy flow injected into the former, but we will investigate this in more detail.

The total intensity I, obtained by integrating the spectra in the wavelength range (2365 to 405 nm), resulted in $I_1 = 3.6 \times 10^{-8}$ W/m^2/sr for Flare 1 and $I_1 = 5.8 \times 10^{-9}$ W/m^2/sr for Flare 2, that is, Flare 1 had a greater total intensity than Flare 2 by a factor of approximately 6.2. As discussed above, this is probably due to the greater amount of energy deposited in Flare 1. However, the other parameters of the electron beam are also relevant, and will be investigated in the continuation of this project.

We also evaluated the temporal evolution of the obtained spectra. Figure 2 shows the result obtained for the evolution of the excess spectra of Flares 1 and 2 in time intervals of five seconds. As expected, Flare 1 presents more intense lines than Flare 2 also throughout the temporal evolution. We highlight here the broadening and asymmetry of the lines in Flare 1, signs of plasma movement in the region where these lines are formed, and affecting the profile of the lines through the Doppler effect (Kuridze et al 2015). As `RADYN` models store information on the macroscopic velocity of the plasma, we will investigate this relationship to verify the diagnostic potential of the plasma movement in future observations.

Acknowledgements. GFSS acknowledges support from CAPES. The authors acknowledge the partial financial support received from FAPESP grants 2018/04055-8 and 2022/15700-7, CNPq grant 150817/2022-3, as well as MackPesquisa funding agency from Universidade Presbiteriana Mackenzie. PJAS acknowledges support from CNPq grants 307612/2019-8 and 305808/2022-2.

References

A. G. Emslie, et al, 2012, ApJ, 759(1):71.
Adam F. Kowalski, et al, 2013, ApJS, 207(1):15.
Adam F. Kowalski, et al, 2017, ApJ, 837(2):125.
Adam F. Kowalski, et al, 2022, ApJ, 928(2):190.
Christopher M. J. Osborne, et al, 2021, ApJ, 917(1):14.
D. F. Neidig, 2021, Sol. Phys., 85(2):285–302.
D. Kuridze, 2015, ApJ, 813(2):125.
H. Uitenbroek, 2001, ApJ, 557(1):389–398.
Hiroyuki Maehara, 2012, Nature, 485(7399):478–481.
J. E. Vernazza, et al, 1981, ApJS, 45:635–725.
J. M. Fontenla, et al, 1983, ApJ, 406:319.
Joel C. Allred, et al, 2005, ApJ, 630(1):573–586.
Joel C. Allred, et al, 2015, ApJ, 809(1):104.
Joel C. Allred, et al, 2020, ApJ, 902(1):16.
Kosuke Namekata, et al, 2017, ApJ, 851(2):91.
L. Fletcher, et al, 2011, Space Sci. Rev., 159(1-4):19–106.
L. Fritzová-Švestková and Z. Švestka, et al, 1967, Sol. Phys., 2(1):87–97.
M. E. Machado, et al, 1974, Sol. Phys., 38(2):499–516.
M. E. Machado, et al, 1980, ApJ, 242:336–351.
Mats Carlsson, et al, 1995, ApJ, 440:L29.
Mats Carlsson, et al, 2023, A&A, 673:A150.
Ondˇrej Procházka, et al, 2017, ApJ, 837(1):46.
P. Kotrˇc, et al, 2016, Sol. Phys., 291(3):779–789.
Paulo J.A. Simões, et al, 2024, mnras, 528(2):2562-2567.
Ryan O. Milligan, et al, 2014, ApJ, 793(2):70.
S. Okamoto, et al, 2022, VizieR Online Data Catalog, art. J/ApJ/906/7.
Suzanne L. Hawley, et al, 1991, ApJ, 378:725.
Suzanne L. Hawley, et al, 2003, ApJ, 597(1):535–554.
Vincenzo Capparelli, et all, 2017, ApJ, 850(1):36.